

Rotational modes in molecular magnets with antiferromagnetic Heisenberg exchange

J. Schnack

*Universität Osnabrück, Fachbereich Physik
Barbarastr. 7, 49069 Osnabrück, Germany*

Marshall Luban

*Ames Laboratory & Department of Physics and Astronomy, Iowa State University
Ames, Iowa 50011, USA*

Abstract

In an effort to understand the low temperature behavior of recently synthesized molecular magnets we present numerical evidence for the existence of a rotational band in systems of quantum spins interacting with nearest-neighbor antiferromagnetic Heisenberg exchange. While this result has previously been noted for ring arrays with an even number of spin sites, we find that it also applies for rings with an odd number of sites as well as for all of the polytope configurations we have investigated (tetrahedron, cube, octahedron, icosahedron, triangular prism, and axially truncated icosahedron). It is demonstrated how the rotational band levels can in many cases be accurately predicted using the underlying sublattice structure of the spin array. We illustrate how the characteristics of the rotational band can provide valuable estimates for the low temperature magnetic susceptibility.

PACS: 75.10.Jm, 75.40.Cx

I. INTRODUCTION AND SUMMARY

The subject of molecular magnets has greatly advanced in recent years due to notable progress in synthesizing bulk samples of identical molecular-size units¹⁻⁴, each containing a relatively small number of paramagnetic ions (“spins”) that mutually interact via Heisenberg exchange. An especially attractive feature of many of these systems is that the intermolecular magnetic interactions are utterly negligible as compared to the intramolecular interactions.

Already at this early stage it is clear that even Heisenberg systems of relatively modest size pose a major theoretical challenge. A stunning example is provided by the recently synthesized molecular magnet⁵ $\{\text{Mo}_{72}\text{Fe}_{30}\}$, where the 30 Fe^{3+} ions (spins $5/2$) occupy the sites of an icosidodecahedron. The total dimension of the Hilbert space for this spin system is a staggering 6^{30} , namely of order Avogadro’s number, utterly precluding the calculation of the energy eigenvalues and eigenvectors on any imagined configuration of immense, ultra-fast computers. This is the context for our exploration in this article of a generic feature of the

low-lying excitation energies of a finite number of spins interacting via antiferromagnetic Heisenberg exchange. With the knowledge of the low-lying excitations one can establish the very low temperature properties and in some cases even arrive at an estimate of the temperature range for the manifestation of essentially quantum behavior. This is illustrated in the present article for $\{\text{Mo}_{72}\text{Fe}_{30}\}$; we arrive at an expression for the temperature dependence of the weak-field susceptibility at very low temperatures. We also provide an estimate for the temperature above which this system can reliably be described by the classical Heisenberg model, a far more practical theoretical platform than the corresponding quantum model. Indeed the classical Heisenberg model is currently being exploited so as to provide detailed quantitative predictions^{6,7} for $\{\text{Mo}_{72}\text{Fe}_{30}\}$ that are being compared to the results of ongoing experiments.⁶

In this article we focus on a generic feature of highly symmetric geometric arrays (ring structures or polytopes) housing a finite number of spins interacting via antiferromagnetic Heisenberg exchange. Whatever the intrinsic spin of the individual paramagnetic ions, or the specific geometrical symmetries of the spin array, there always exist what we refer to as rotational modes. Besides their intrinsic interest, we show that the knowledge of these modes can in many cases be used to obtain good estimates of physical observables, such as the magnetic susceptibility at very low temperatures. We consider in the following a finite number, N , of quantum spins, each of intrinsic spin s , that in most examples interact via nearest-neighbor isotropic Heisenberg exchange. We assume that all nearest-neighbor pairs of spins interact with the same coupling constant, one which favors antiferromagnetic ordering. If \vec{S} denotes the total spin operator, the operator \vec{S}^2 commutes with the Hamilton operator, and thus we can structure the set of all energy eigenvalues according to the total spin quantum number S , extending up to $S_{\text{max}} = Ns$. A key point of the present work relates to the subset of minimal energies for the allowed values of S . We may summarize our findings as follows: *Whatever the details of the system, this subset of minimal energies appears to define what we shall refer to as a “rotational band”, i.e., is well approximated by a dependence on S of the form $S(S+1)$.* We choose the term “rotational band” to indicate that this portion of the spectrum is similar to that of a rigid rotor. Similar behavior is commonly found also in nuclear and atomic physics.

The occurrence of a rotational band has been noted on several occasions for an even number of spins defining a ring structure. The minimal energies have been described^{8–11} as “following the Landé interval rule”. However, we find that the same property also occurs for rings with an odd number of spins as well as for the various polytope configurations we have investigated, in particular for quantum spins positioned on the vertices of a tetrahedron, cube, octahedron, icosahedron, triangular prism, and an axially truncated icosahedron. Rotational modes have also been found in the context of finite triangular lattices of spin-1/2 Heisenberg antiferromagnets^{12,13}.

Using only the sublattice structure of the various spin arrays, which is provided by symmetry arguments, we are able to approximate the coefficient of the $S(S+1)$ dependence to good accuracy. Our method describes in general how this approximate coefficient can be deduced. We can therefore obtain an estimate of the ground state energy as well as the low-lying rotational excitations. It is clear that at low temperatures these minimal energies provide the major contribution to thermal averages. This enables us to discuss the low-temperature behavior of quantities such as the magnetic susceptibility without knowledge

of the complete eigenvalue spectrum. We illustrate these considerations for the special case of $\{\text{Mo}_{72}\text{Fe}_{30}\}$.

The layout of this article is as follows. In Sec. II we present our numerical findings for various Heisenberg spin systems and motivate in Sec. III how the rotational band is connected to the topology of spin sites. Finally in Sec. IV we discuss some implications of the rotational band on physical observables.

II. ROTATIONAL BANDS

The Hamilton operator for the isotropic Heisenberg model in the absence of an external magnetic field reads

$$\underline{H} = -2J \sum_{(u,v)} \underline{\vec{s}}(u) \cdot \underline{\vec{s}}(v) , \quad \forall u : s(u) = s , \quad (1)$$

where J is the exchange interaction with units of energy, and $J < 0$ results in antiferromagnetic coupling. The vector operators $\underline{\vec{s}}(u)$, underlined with a tilde, are the single-particle spin operators with eigenvalue equations

$$\begin{aligned} \left(\underline{\vec{s}}(u) \right)^2 |s(u) m(u)\rangle &= s(s+1) |s(u) m(u)\rangle \\ \underline{s}_z(u) |s(u) m(u)\rangle &= m(u) |s(u) m(u)\rangle . \end{aligned} \quad (2)$$

The sum in (1) runs over all distinct interacting pairs (u, v) of spins at positions u and v . For a closed ring with nearest-neighbor interaction the index v would simply equal $u + 1$ and the sum is understood to fulfill the cyclic boundary condition.

A. Heisenberg square

One of the few systems that possesses a rigorous parabolic rotational band is the Heisenberg square, i.e., a ring with $N = 4$. Because the Hamilton operator can be rewritten as

$$\underline{H} = -J \left(\underline{\vec{s}}^2 - \underline{\vec{s}}_{13}^2 - \underline{\vec{s}}_{24}^2 \right) , \quad \underline{\vec{s}}_{13} = \underline{\vec{s}}(1) + \underline{\vec{s}}(3) , \quad \underline{\vec{s}}_{24} = \underline{\vec{s}}(2) + \underline{\vec{s}}(4) , \quad (3)$$

with all spin operators $\underline{\vec{s}}^2$, $\underline{\vec{s}}_{13}^2$ and $\underline{\vec{s}}_{24}^2$ commuting with each other and with \underline{H} , one can directly obtain the complete set of eigenenergies and these are characterized by the quantum numbers S , S_{13} and S_{24} . In particular, the lowest energy for a given total spin quantum number S occurs for the choice $S_{13} = S_{24} = 2s$

$$E_{S,min} = -J [S(S+1) - 2 \cdot 2s(2s+1)] = E_0 - J S(S+1) , \quad (4)$$

where $E_0 = 4s(2s+1)J$ is the exact ground state energy. The various energies $E_{S,min}$ form a rigorous parabolic rotational band of excitation energies. Therefore, these energies coincide with a parabolic fit (crosses connected by the dashed line on the l.h.s. of Fig. 1) passing through the antiferromagnetic ground state energy and the highest energy level, i.e., the ground state energy of the corresponding ferromagnetically coupled system.

B. Heisenberg rings with $N > 4$

We have calculated all energy levels by diagonalizing¹⁴ the Hamilton matrix for a variety of rings with different values of N and s . All of these systems exhibit a rotational band, irrespective whether N is even or odd and for both integer and half-integer values of s . That is, the subset of minimal energies is well approximated by a dependence on S which is proportional to $S(S+1)$, i.e., follows the Landé interval rule⁸⁻¹¹,

$$E_{S,min} \approx E_a - J \frac{D(N, s)}{N} S(S+1) . \quad (5)$$

We determine the parameters E_a and $D(N, s)$ so that formula (5) reproduces our calculated values of the lowest and highest energies of the rotational band, i.e., the ground state energy of the antiferromagnetic system and the ground state energy of the corresponding ferromagnetic system. In all cases we have observed, that if deviations occur the fitting parabola of (5) lies below the rotational band. Use of (5) is illustrated in Fig. 1 (r.h.s.) for the case $N = 6$ and $s = 3/2$. The figure shows the complete spectrum (horizontal dashes) as well as the fit according to (5) (crosses connected by a dashed line). One observes that the fit very nearly matches the energies of the rotational band, meaning that the Landé interval rule is obeyed with high accuracy. As a second example, spectra are shown for rings of five spins with $s = 2$ (Fig. 2, l.h.s.) and $s = 5/2$ (Fig. 2, r.h.s.). Inspecting the low-lying excitations one notices that the rotational band for odd rings is not separated from the remaining states as much as it is for even rings. This remark also pertains to other, larger odd values of N .

In Table I we collect the coefficients $D(N, s)$ for the rings we have investigated. In all cases $D(N, s) \approx 4$. For the odd rings the values of $D(N, s)$ may be somewhat smaller than four. We will dwell on this fact in Sec. III.

It should be noted that in the large- N -limit the rotational levels (5) become degenerate since $D(N, s)$ remains finite. Therefore, excitations within the rotational band should not be confused with magnons.

C. Frustrated spin rings

Even for spin rings with next-nearest neighbor interaction the rotational band persists. The energy spectra of Fig. 3 have been calculated for the Hamilton operator

$$\tilde{H} = -2 J_{nn} \sum_{u=1}^N \vec{\tilde{s}}(u) \cdot \vec{\tilde{s}}(u+1) - 2 J_{nnn} \sum_{u=1}^N \vec{\tilde{s}}(u) \cdot \vec{\tilde{s}}(u+2) , \quad (6)$$

where all spins have been taken to be $s(u) = 3/2$. In Fig. 3 we display spectra for a ring with $N = 6$ and $s = 3/2$ for various ratios of the two coupling constants J_{nn} and J_{nnn} . Although details of the spectra differ, the overall appearance persists, and in particular the minimal energies define a rotational band.

D. Heisenberg polytopes

In order to illustrate the generality of the rotational band we provide several additional examples, the tetrahedron, the cube (Fig. 4), the octahedron (Fig. 5, l.h.s.), and the icosahedron (Fig. 5, r.h.s.). As in the previous cases the displayed energy eigenvalues are calculated by numerical diagonalization, except for the tetrahedron and octahedron which can be solved analytically.

The tetrahedron of spins is a worthy textbook problem; it can be solved with a few lines of algebra because the Hamilton operator simplifies to

$$\tilde{H} = -J \left(\tilde{\vec{S}}^2 - 4 \tilde{\vec{s}}^2 \right) . \quad (7)$$

Therefore, the spectrum of this system consists exclusively of a rotational band.

The case of the octahedron is similar to the Heisenberg square; the Hamilton operator can be written as

$$\tilde{H} = -J \left(\tilde{\vec{S}}^2 - \tilde{\vec{S}}_A^2 - \tilde{\vec{S}}_B^2 - \tilde{\vec{S}}_C^2 \right) , \quad (8)$$

where $\tilde{\vec{S}}_A$, $\tilde{\vec{S}}_B$, $\tilde{\vec{S}}_C$ are the sums for pairs of spins situated at opposite vertices of the octahedron, and $\tilde{\vec{S}}$ is the total spin. The spin operators $\tilde{\vec{S}}^2$, $\tilde{\vec{S}}_A^2$, $\tilde{\vec{S}}_B^2$ and $\tilde{\vec{S}}_C^2$ commute with each other and with \tilde{H} . Thus the eigenvalues of \tilde{H} may be written down at once and they are given in terms of the quantum numbers S , S_A , S_B and S_C . Therefore, the lowest energy for a given value of S is achieved if $S_A = S_B = S_C = 2s$, and its value is given by

$$E_{S,min} = -J [S(S+1) - 3 \cdot 2s(2s+1)] . \quad (9)$$

This is another one of the few cases where the minimal energies define a rigorous rotational band (see Fig. 5, l.h.s.).

The remaining examples of the cube (Fig. 4) and the icosahedron (Fig. 5, r.h.s.) illustrate the behavior of the gaps between the rotational band and the remaining eigenenergies. It is worth noting that the rotational band of the icosahedron is not as well separated from higher energy levels as it is for the cube. This behaviour is similar to that discussed above for even and odd rings. Systems which are bipartite, i.e., can be subdivided into two sublattices with interactions only between spins of different sublattices (rings with even N and the cube), show a significant gap, whereas systems, that are non-bipartite appear to show much smaller gaps.¹⁵ The latter systems are often also called frustrated.¹⁶ Two other cases we have studied, the equilateral triangle prism and an axially truncated icosahedron, conform with these trends.

III. CONJECTURE ON ROTATIONAL BANDS

A. Heisenberg rings; even N

It turns out that an accurate approximate formula for the coefficient $D(N, s)$ of (5) can be developed using the sublattice structure of the spin array. As an introductory example

we repeat the basic ideas for Heisenberg rings with an even number of spin sites¹¹. Such rings are bipartite and can be decomposed into two sublattices, labeled A and B , with every second spin belonging to the same sublattice. From classical spin dynamics it is known that the classical ground state, sometimes called the classical Néel state¹², is given by an alternating sequence of opposite spin directions. On each sublattice the spins are mutually parallel. Therefore, a quantum trial state, where the individual spins on each sublattice are coupled to their maximum values, $S_A = S_B = Ns/2$, could be expected to provide a reasonable approximation to the true ground state, especially if s assumes large values. Such trial states are called Néel-like. For rings with even N the approximation to the respective minimal energies for each value of the total spin $\vec{S} = \vec{S}_A + \vec{S}_B$ is found to be given by¹¹

$$E_{S,min}^{\text{approx}} = -\frac{4J}{N} \left[S(S+1) - 2\frac{Ns}{2} \left(\frac{Ns}{2} + 1 \right) \right]. \quad (10)$$

This approximation exactly reproduces the energy of the highest energy eigenvalue, i.e., the ground state energy of the corresponding ferromagnetically coupled system ($S = Ns$), since the true eigenstate with all spins assuming their largest m quantum number, $m = s$, is a linear combination of Néel-like states. For all smaller S the approximate minimal energy $E_{S,min}^{\text{approx}}$ is bounded from below by the true one (Rayleigh-Ritz variational principle). The solid curve displays this behavior for the example of $N = 6$, $s = 3/2$ in Fig. 1 (r.h.s.). The entries in Table I provide additional numerical support for the approximation $D(N, s) \approx 4$ adopted in (10). For each fixed even N the coefficient $D(N, s)$ approaches 4 with increasing s .

The approximate spectrum, (10), is similar to that of two spins, \vec{S}_A and \vec{S}_B , each of spin quantum number $Ns/2$, that are coupled by an effective interaction of strength $4J/N$. Therefore, one can equally well say, that the approximate rotational band considered in (10) is associated with an effective Hamilton operator

$$\tilde{H}^{\text{approx}} = -\frac{4J}{N} \left[\vec{S}^2 - \vec{S}_A^2 - \vec{S}_B^2 \right], \quad (11)$$

where the two sublattice spins, \vec{S}_A, \vec{S}_B , assume their maximal value $S_A = S_B = Ns/2$. This result agrees with that obtained by a different procedure, which utilizes a Fourier representation of the Hamilton operator.¹²

In retrospect one realizes that all we needed for rings with even N to arrive at (10) was a sublattice structure in order to build Néel-like trial states. The sublattice structure can be deduced from the classical ground state or the symmetries of the spin array, which manifest themselves in the classical ground state. In the case of rings with an even number of sites the symmetry is the cyclic shift symmetry: Sublattice A can be transformed into sublattice B by a single shift. These considerations lead us in the following subsection to a generalization for other systems.

B. Conjecture

We assume that the Heisenberg spin system can be decomposed into N_{sl} sublattices according to a symmetry transformation. The spins of each sublattice are to be coupled to

their maximal values $S_{sl} = Ns/N_{sl}$. Then we conjecture that the energies of the rotational band can be approximated as

$$E_{S,min}^{\text{approx}} = -J \frac{D}{N} [S(S+1) - N_{sl} S_{sl}(S_{sl}+1)] , \quad (12)$$

where the parameter D is to be fixed by the requirement that the energy $E_{\text{ferro}} = -2J N_b s^2$ of the corresponding ferromagnetic ground state, for which $S = Ns$, is reproduced exactly. The energy E_{ferro} depends only on the number of distinct bonds N_b . Therefore, the coefficient D is given by

$$D = 2 \frac{N_b}{N} \frac{1}{1 - \frac{1}{N_{sl}}} , \quad (13)$$

which is independent of s . For rings with an even number of sites this formula reproduces the value $D = 4$, whereas for the cube, which has $N_b = 12$, it gives $D = 6$. That these values of D provide a very good estimate of the coefficients $D(N, s)$ is demonstrated in Fig. 1 (r.h.s.) for a ring with $N = 6$ and $s = 3/2$, and in Fig. 4 for cubes with $s = 1$ and $s = 3/2$.

If there are several possible partitions into sublattices according to various symmetries of the spin array one can safely choose that one which leads to the lowest approximate ground state energy, because this energy is bounded from below by the true ground state energy. For spin arrays with low symmetry the gained approximation can be rather poor. This is for instance the case for rings of odd N . The classical ground state structure would suggest as many sublattices as spin sites, which leads to rather small coefficients D as depicted in Table I (“simple conjecture”). A closer inspection shows that it is possible to obtain a better approximation if one defines the approximate rotational band by the parabola passing through the classical Néel ground state energy level and through the ground state energy level of the corresponding ferromagnetic system. For rings of odd N the classical Néel ground state energy is

$$E_{\text{Néel}} = -2 J N s^2 \cos((N-1)\pi/N) , \quad (14)$$

as can be shown using spin coherent states.¹⁷ This leads to the “refined conjecture” for odd rings, see Table I. For other spin arrays, such as the icosahedron, it may be simply impossible to derive a good approximation for the coefficient $D(N, s)$, nevertheless, the minimal energies always form a rotational band according to (5).

Using (12) and (13) one can find an approximation for the rotational band for larger polytopes such as the icosidodecahedron, which characterizes the sites of the 30 paramagnetic Fe^{3+} ions in the recently synthesized molecular magnet⁵ $\{\text{Mo}_{72}\text{Fe}_{30}\}$. The related Hilbert space has a dimension of $(2s+1)^N = 6^{30}$ which is of the order of Avogadro’s number. Numerical diagonalization of the Hamilton matrix is totally out of reach. Nevertheless, we can estimate both the ground state energy and the form of the rotational band. The icosidodecahedron, consisting of 20 triangles and 12 pentagons, has threefold rotational symmetry and thus three sublattices. Assuming nearest neighbor interaction, we have $N_b = 60$. Thus, one ends up with

$$E_{S,min}^{\text{approx}} = -\frac{J}{5} S(S+1) + 60Js \left(s + \frac{1}{10} \right) . \quad (15)$$

The threefold rotational symmetry of the spin array is also reflected by the structure of the classical ground state, thus it is no surprise that quantum and classical Néel ground state energies,

$$E_{0,min}^{\text{approx}} = 60Js(s + 1/10) \quad , \quad E_{\text{Néel}} = 60Js^2 \quad , \quad (16)$$

differ from each other only by 4% for the rather high $s = 5/2$.

IV. LOW-TEMPERATURE THERMODYNAMIC PROPERTIES

It is obvious that at low temperatures the rotational band energies provide the dominant contribution to thermal averages, especially if these energies are well separated from the remaining energy levels. This suggests, for example, that we approximate the partition function by

$$Z(\beta) \approx \sum_{S=S_{min}}^{S_{max}} d_S e^{-\beta[E_a - J \frac{D}{N} S(S+1)]} \quad , \quad (17)$$

where d_S is the degeneracy factor of the eigenenergies belonging to the rotational band, and $E_a = J(D/N) N_{sl} S_{sl}(S_{sl} + 1)$ according to (12). For bipartite systems, i.e. systems that can be subdivided into two sublattices according to the theorem of the Lieb-Schultz-Mattis^{18,19}, $d_S = 2S + 1$. For non-bipartite systems not much is known about the degeneracy. First investigations show that it is possible to establish rules for the degeneracy of certain states also for non-bipartite systems.²⁰ For the approximate rotational energies we take the degeneracies to be that resulting from the coupling of the sublattice spins.¹² It might be that the full Hamiltonian lifts this degeneracy somewhat, nevertheless this procedure provides a reasonable approximation for the degeneracies of the true minimal energies.

The corresponding approximation of the zero-field susceptibility is then given by

$$\chi_0 \approx \frac{g^2 \mu_B^2 \beta}{Z} \sum_{S=S_{min}}^{S_{max}} \frac{d_S}{2S+1} \left(\sum_{M=-S}^{M=S} M^2 \right) e^{-\beta[E_a - J \frac{D(N,s)}{N} S(S+1)]} \quad . \quad (18)$$

Inspecting Fig. 6 one sees how the rotational band contributes to the susceptibility in the case of the ring with $N = 6$ and $s = 5/2$. The rise at low temperatures is mostly determined by the first excited level of the rotational band (dashed curve labeled 1).

As our final example we show in Fig. 7 the result using (15) and (18) for the low temperature behavior of the zero-field susceptibility for $\{\text{Mo}_{72}\text{Fe}_{30}\}$. For this system $d_s = \min\{(2S+1)^2, (2S+1)(76-S)\}$. The susceptibility (solid curve) rises very rapidly with increasing temperature to the result²¹ for the classical Heisenberg model (dash-dot curve). Inspecting (15) one can understand that the rapid rise is due to the small energy difference between ground and first excited state and in particular because of the small coefficient $J/5$ of the $S(S+1)$ term. In addition the $S = 1$ level of the approximate rotational band is 9-fold degenerate and thus the rapid rise in χ_0 commences at very low temperatures. Thus, for $\{\text{Mo}_{72}\text{Fe}_{30}\}$, which has a nearest neighbor coupling constant⁶ of $J/k_B \approx 0.75$ K, we expect, that weak-field susceptibility measurements will confirm the rapid decrease on cooling, which is a genuine quantum feature and not present in the classical counterpart, only at temperatures below $T \approx 0.15$ K.

ACKNOWLEDGMENTS

The authors thank A. Cornia (Modena), D. Gatteschi (Florence), and M. Karbach (Wuppertal) for helpful discussions and J. Richter (Magdeburg) for drawing their attention to the work of C. Lhuillier. We are deeply indebted to our collaborator C. Schröder (Telelogic GmbH, Bielefeld) for innumerable discussions and quantitative results. We also thank DAAD and NSF for supporting a mutual exchange program. The Ames Laboratory is operated for the United States Department of Energy by Iowa State University under Contract No. W-7405-Eng-82.

REFERENCES

- * Email: jschnack@uos.de, luban@ameslab.gov
- ¹ R. Sessoli, D. Gatteschi, and A. Caneschi, *Nature* (London) **365**, 141 (1993).
- ² A. Caneschi and L. Pardi, *Science* **265**, 1054 (1994).
- ³ D. Gatteschi, *Adv. Mat.* **6**, 635 (1994).
- ⁴ *Localized and Itinerant Molecular Magnetism: From Molecular Assemblies to the Devices*, Vol. 321 of *NATO Advanced Study Institute, Series E: Applied Sciences*, edited by E. Coronado *et al.* (Kluwer Academic, Dordrecht, 1996).
- ⁵ A. Müller, S. Sarkar, S.Q.N. Shah, H. Bögge, M. Schmidtman, Sh. Sarkar, P. Kögerler, B. Hauptfleisch, A.X. Trautwein, and V. Schünemann, *Angew. Chem. Int. Ed.* **38**, 3238 (1999).
- ⁶ A. Müller, M. Luban, C. Schröder, R. Modler, P. Kögerler, M. Axenovich, J. Schnack, P.C. Canfield, and S. Bud'ko, *Nature* (submitted).
- ⁷ C. Schröder and M. Luban, (unpublished).
- ⁸ K.L. Taft, C.D. Delfs, G.C. Papaefthymiou, S. Foner, D. Gatteschi, and S.J. Lippard, *J. Am. Chem. Soc.* **116**, 823 (1994).
- ⁹ A. Lascialfari, D. Gatteschi, F. Borsa, and A. Cornia, *Phys. Rev. B* **55**, 14341 (1997).
- ¹⁰ A. Lascialfari, D. Gatteschi, F. Borsa, and A. Cornia, *Phys. Rev. B* **56**, 8434 (1997).
- ¹¹ G. L. Abbati, A. Caneschi, A. Cornia, A. C. Fabretti, and D. Gatteschi, *Inorganic Chimica Acta* **297**, 291 (2000).
- ¹² B. Bernu, P. Lecheminant, C. Lhuillier, and L. Pierre, *Phys. Rev. B* **50**, 10048 (1994).
- ¹³ M. Gross, E. Sánchez-Velasco, and E.D. Siggia, *Phys. Rev. B* **40**, 11328 (1989).
- ¹⁴ K. Bärwinkel, H.-J. Schmidt, and J. Schnack, *J. Mag. Mag. Mater.* **212**, 240 (2000).
- ¹⁵ A. Voigt, J. Richter, and P. Tomczak, *J. Mag. Mag. Mater.* **183**, 68 (1998).
- ¹⁶ J. Richter, N.B. Ivanov, A. Voigt, and K. Retzlaff, *J. Low Temp. Phys.* **99**, 363 (1995).
- ¹⁷ E.H. Lieb, *Commun. math. Phys.* **31**, 327 (1973).
- ¹⁸ E. Lieb, T. Schultz, and D. Mattis, *Ann. Phys. (N.Y.)* **16**, 407 (1961).
- ¹⁹ E. Lieb and D. Mattis, *J. Math. Phys.* **3**, 749 (1962).
- ²⁰ J. Schnack, *Phys. Rev. B* (accepted).
- ²¹ M. Axenovich and M. Luban (in preparation).

TABLES

s	N						
	5	6	7	8	9	10	
	2.5	4	2.333	4	3	4	simple conjecture
	3.618	4	3.802	4	3.879	4	refined conjecture
$\frac{1}{2}$	3.8975	4.3028	4.2982	4.5209	4.5355	4.6770	
1	3.8437	4.1764	4.1430	4.2971	4.2957	4.3809	
$\frac{3}{2}$	3.7591	4.1190	4.0174	4.1977	4.1443	4.2514	
2	3.7399	4.0896	3.9772	4.1482	4.0886	4.1881	
$\frac{5}{2}$	3.7103	4.0718	3.9368	4.1185	4.0420	4.1500	

TABLE I. Coefficients $D(N, s)$ for various Heisenberg rings, to be used in conjunction with (5).

FIGURES

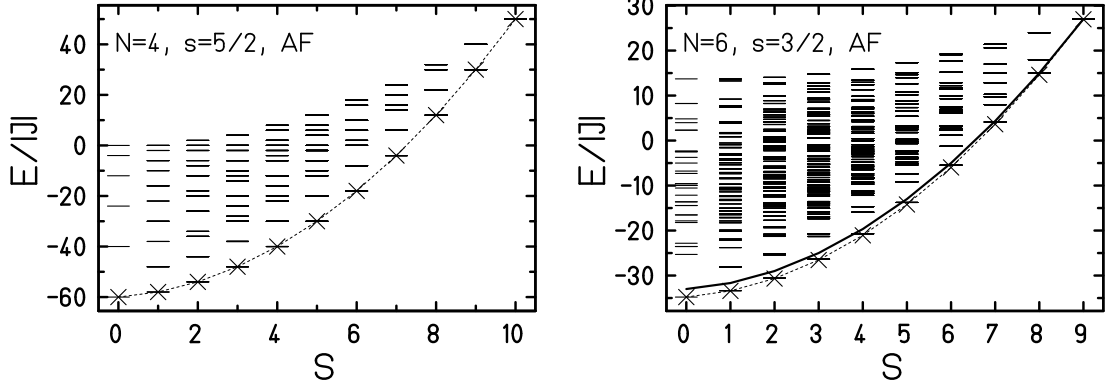


FIG. 1. Energy spectra of antiferromagnetically coupled Heisenberg spin rings (horizontal dashes). Here and in all subsequent figures the crosses connected by the dashed line always represent the fit to the rotational band according to (5), which by definition matches both the lowest and the highest energies exactly. On the l.h.s the dashed line reproduces the exact rotational band, whereas on the r.h.s. it only approximates it, but to high accuracy. The solid line on the r.h.s. corresponds to the approximation of (10).

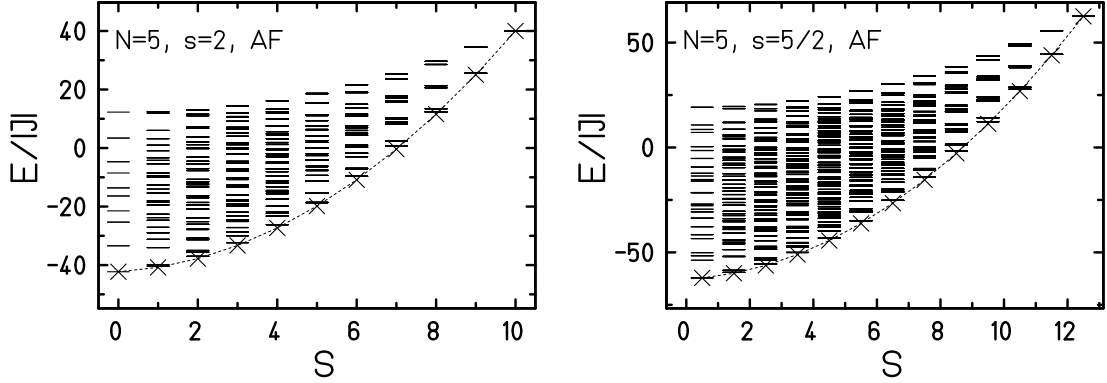


FIG. 2. Energy spectra of antiferromagnetically coupled Heisenberg spin rings with $N = 5$, $s = 2$ (l.h.s.) and $s = 5/2$ (r.h.s.).

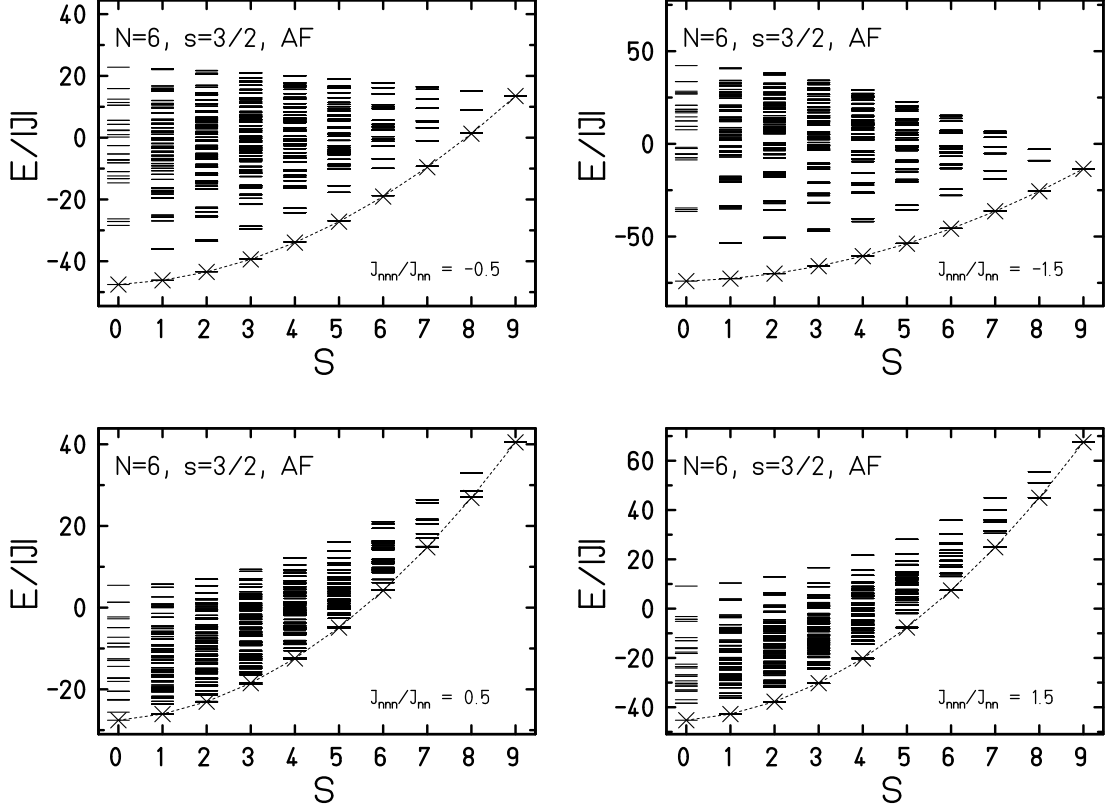


FIG. 3. Energy spectrum of an antiferromagnetically next neighbor coupled Heisenberg ring with competing next-nearest neighbor interaction.

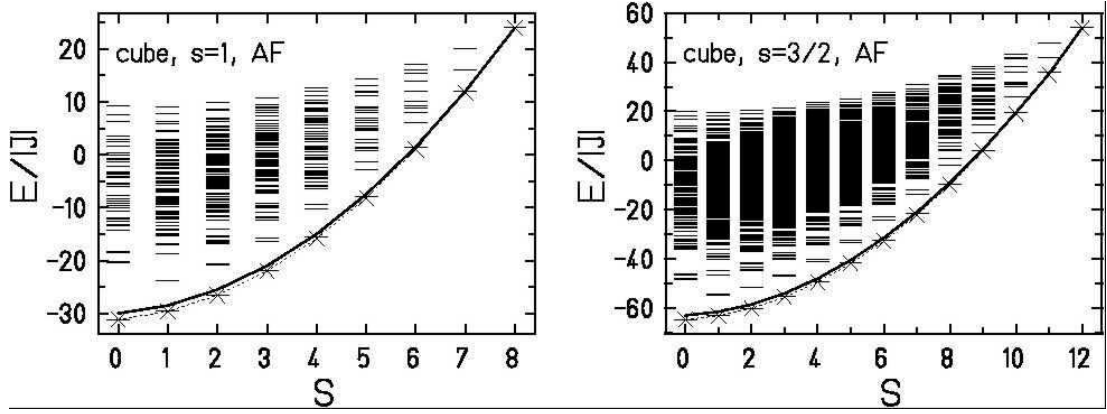


FIG. 4. Energy spectrum of antiferromagnetically coupled Heisenberg cubes. The solid lines correspond to the approximation of (12) and (13), i.e. $D = 6$.

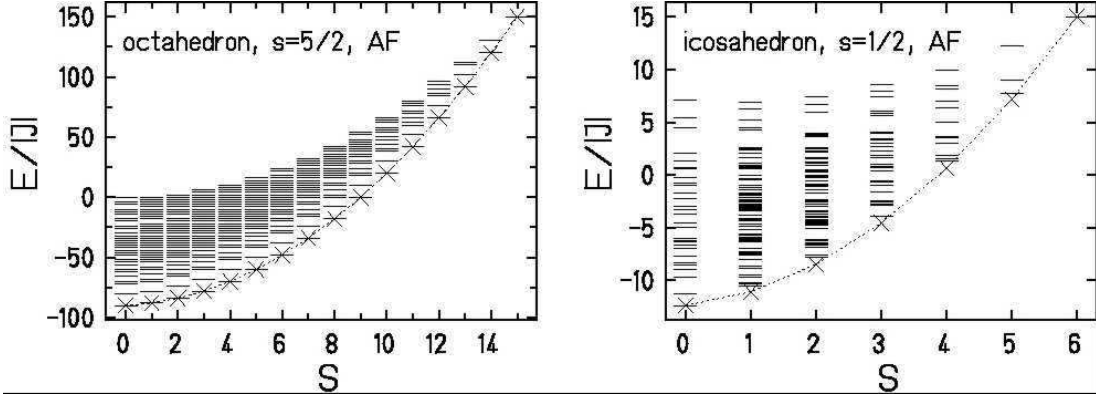


FIG. 5. Energy spectrum of an antiferromagnetically coupled Heisenberg octahedron (l.h.s.) and icosahedron (r.h.s.).

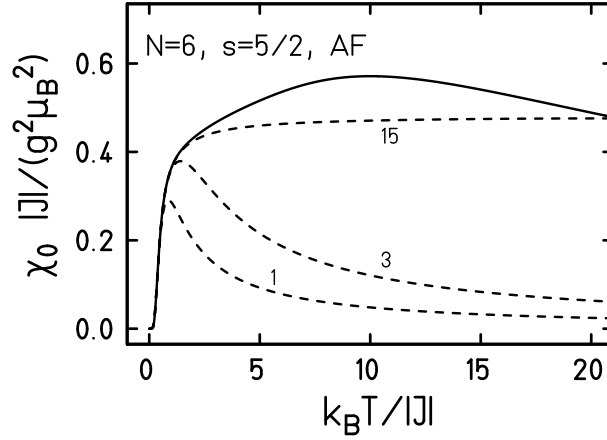


FIG. 6. Zero-field magnetic susceptibility of the antiferromagnetically coupled Heisenberg spin ring with $N = 6$ and $s = 5/2$. The solid curve displays the full quantum solution; the dashed curves correspond to approximation (18) upon including the contributions of rotational levels up to $S = 1$, $S = 3$, and $S = 15$.

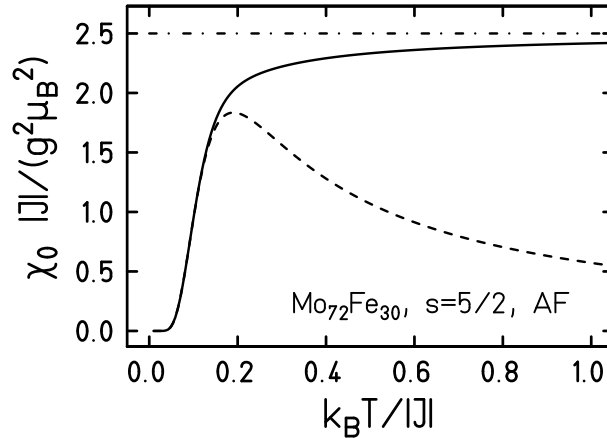


FIG. 7. Zero-field magnetic susceptibility of $\{\text{Mo}_{72}\text{Fe}_{30}\}$ calculated using (15) and (18). The dashed curve is obtained using only the two lowest levels and the solid curve using all levels of the approximate rotational band. The classical result is given by the dash-dot line.